Robotic Multiaxial Testing and Constitutive Characterization of Composites

J.G. Michopoulos,[1] J.C. Hermanson,[2] and A. Iliopoulos[3]
[1]*Materials Science and Technology Division*
[2]*Forest Products Laboratory, USDA Forest Service*
[3]*George Mason University*

Introduction: Determining the constitutive response of polymer matrix composite materials is a critical requirement for using such materials in naval applications. This information is essential to structural design, material qualification and certification, material manufacturing, maintainability, and structural health monitoring. Over the past decade, we have been engaged in an effort to automate both the massive multiaxial testing of composite coupons required for constitutive characterization and the computational methodologies required for extracting the constitutive response from these tests. Here we report on the completion of the first recursively defined, custom-made, hexapod testing machine, capable of 6-degree-of-freedom (6-DoF) tests, and the first high-throughput, data-driven campaign of experiments for the purpose of constitutive characterization. Our approach is motivated by the data-driven requirements of employing design optimization principles for determining the constitutive behavior of composite materials.[1]

NRL66.3 – NRL's Robotic Multiaxial Testing System: NRL's work in developing multi-degree-of-freedom automated mechatronic testing machines in conjunction with energy-based inverse characterization methodologies has culminated in the most recent advanced system, named NRL66.3, shown in Fig. 1(a). The NRL66.3 system has a recursive character; it has a hexapod configuration that is repeated six times. Details of the design reasoning, architecture, systemic requirements, and hardware and software prototyping are provided elsewhere.[2] The most critical recursion of this hexapod consists of the assembly connecting the bottom and top star-shaped frames with six linear actuators that are digitally controlled, through six spherical joints, which is known to the parallel robots community as a 6-6p parallel linkage mechanism. This configuration enables the conversion of the linear motion of the six actuators to the 6-DoF motion of a movable platform (upper section of the system with the associated upper grip). This motion corresponds to the three translations along the axes of an orthogonal Cartesian system located in the midpoint of the specimen between the grips, and three rotations about the same three axes. Therefore, a specimen gripped between the two grips as depicted in Fig. 1(b,c) can be tested in a loading path defined by the evolution of any linear combination of these six motions, resulting in the most general possible multiaxial state of loading.

The other associated recursions consist of hexapods that contain in-line displacement and force sensors instead of linear actuators. Another critical feature of the system is the integration of two pairs of stereoscopic machine vision systems, custom developed for implementing the in-house developed full field displacement and strain measurement method known as Meshless (or Mesh Free) Random Grid Method (MRGM).[3] Two additional collaborating serial robotic systems are used in a synergistic manner for inserting and extracting the specimens into and out of the grips before and after each testing sequence along a predefined loading path.

Computational Implementation of Constitutive Characterization: For the general case of a composite material system, we consider that a modified anisotropic hyperelastic strain energy density function can be constructed to encapsulate both the elastic and the inelastic responses of the material. However, certain classes of composite materials reach failure after small strains and some under large strains. For this reason, we developed two formalisms, one involving a small (infinitesimal) strain energy density (SSED) and another involving a finite (large) strain energy density (FSED). The material parameters to be determined are 9 elastic constants and potentially 12 damage constants, a total of 21.

To determine the material parameters that define the constitutive response, the inverse problem at hand is solved through a design optimization approach described by the iterative logic depicted in Fig. 2. The implementation of this logic employs a computational infrastructure controlled by a Matlab application, where the forward solution of the instantaneous finite element analysis (FEA) was accomplished by a computational customization and parallelization of the ANSYS commercial package.

The objective functions required for the optimization were constructed to express the difference between experimentally measured quantities and their analytical counterpart as predicted from the constitutive model under characterization. The required experimental values of the strains were measured via the REMDIS-3D software,[3] developed by our group; one can obtain full field measurements of the displacement and strain fields over any deformable body. Thus, our experimental measurements for the formation of the objective functions were chosen to be the strains at the nodal points of the FEM discretization. The selected objective functions were implemented in Matlab, and we used a global Monte Carlo optimizer for determining the material parameters.

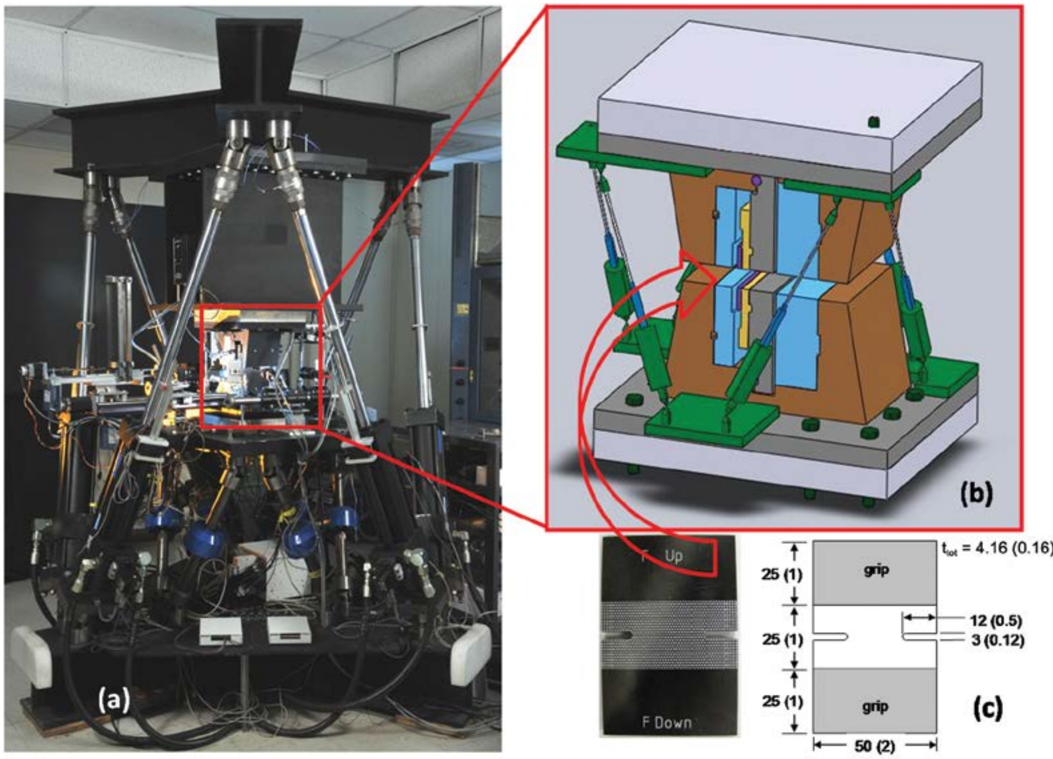

FIGURE 1
(a) View of the NRL66.3, a 6-DoF mechatronically automated system for the multiaxial testing of composite materials; (b) schematic representation of the grip assembly; (c) typical specimen view with specifications in mm (inches).

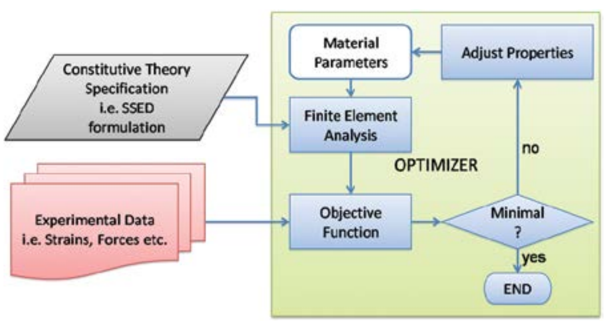

FIGURE 2
Computational design optimization logic overview.

Experimental Campaign: We found that 72 proportional loading paths are required to sample homogeneously the 6-DoF space defined by the three translations and three rotations that can be applied by the moveable grip of the NRL66.3. We used a single specimen per loading path and then repeated the process, requiring 144 specimens per material system. Each material system was a balanced laminate with an alternating angle of fiber inclination per ply relative to the vertical axis of the specimen, which is perpendicular to the axis defined by the two notches of the specimen. Four angles were used (±15, ±30, ±60, ±75 degrees), leading to 4 × 144 = 576 specimens. The material was an AS4/3506-1 epoxy resin/fiber, the original material used for Navy's F/A-18 Hornet platform. Additional considerations raised the final specimen total to 1152. All specimens were tested using NRL66.3 on its inaugural run in May/June 2011. All tests were completed in 12 work days; peak throughput was 28 tests/hour. An example of the testing process can be viewed at http://www.youtube.com/watch?v=Cp18y3HAqsM. The tests yielded 13 TB of data from the sensors and cameras of the system. Using the collected data and the optimization approach outlined above for the case of the SSED, we identified all the material constants.

By applying FEA for the cases that correspond to the specific loading path corresponding to a particular test, we compared the predicted distribution of any component of the strain or stress tensor to the experimental one. To demonstrate how well our identified constitutive model can capture the behavior of the coupons used to obtain the data used in the characterization process, we present in Fig. 3 a typical example of the distribution of ε_{yy} (strain) as measured by the MRGM (left column) and as predicted by the FSED theory (right column), for both the front (top row) and back (bottom row) of a specimen. The observed deviation between predicted and experimental strains never exceeded 3.5%.

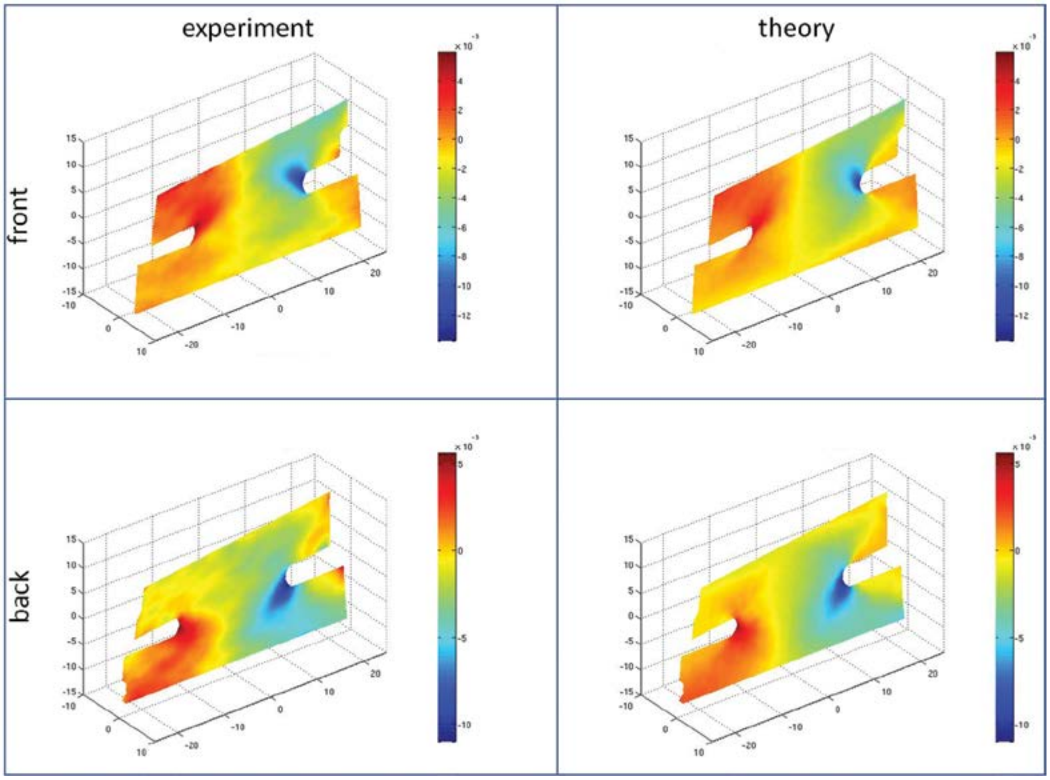

FIGURE 3
Comparison of ε_{yy} strain field as measured (left column) and as predicted by the identified model (right column) for the case of in-plane rotation and torsion of a ±60 degree laminate for both the front side (top row) and the back side (bottom row) of a specimen.

Conclusions: The success of this approach provides closure to the problem of determining the constitutive response of anisotropic materials such as polymer matrix composites used in naval platforms. This approach opens the door for a new and fundamentally different look at the design of composite structures and the associated applications. The derived constitutive response is intrinsically validated because it is based on the measured multiaxial response of the material of interest. The potential for economic and optimally tailored designs of the future is limitless.

[Sponsored by ONR and the NRL Base Program (CNR funded)]

References

[1] J.G. Michopoulos, J.C. Hermanson, A. Iliopoulos, S.G. Lambrakos, and T. Furukawa, "Data-Driven Design Optimization for Composite Material Characterization," *J. of Computing and Information Science in Engineering* **11**(2), 1–10 (2011).

[2] J.G. Michopoulos, J.C. Hermanson, and A. Iliopoulos,"Towards a Recursive Hexapod for the Multidimensional Mechanical Testing of Composites," Proceedings of the ASME 2010 International Design Engineering Technical Conferences and Computers and Information in Engineering Conference, no. DETC2010/CIE-28699, pp. 91–99 (2010).

[3] J.G. Michopoulos and A. Iliopoulos, "A Computational Workbench for Remote Full Field 3D Displacement and Strain Measurements," Proceedings of the ASME 2011 International Design Engineering Technical Conferences and Computers and Information in Engineering Conference IDETC/CIE, August 29–31, 2011, Washington, DC, Vol. 2, pp. 489–498.

♦

How Clutter and Expertise Affect Search in Geospatial Displays

M.E. Trenchard[1] and M.R. Beck[2]
[1]*Marine Geosciences Division*
[2]*Louisiana State University*

Introduction: Clutter and expertise play significant roles in the search performance of users viewing complex geospatial displays.[1,2] As geospatial displays become more complex in a networked battlespace environment, it is critical in both the design and assessment of these displays to ensure that warfighter performance is optimized. Using a quantitative measure of clutter (NRL's Color-Clustering Clutter (C3) algorithm[1]), we can obtain a better understanding of how expertise affects performance at varying levels of clutter and use this information to assess geospatial display systems and improve training doctrine. Clutter may be measured both on a global basis (whole image), which relates favorably to set size (i.e., the number of distractors), and locally (area very near the target), which relates favorably to crowding effects. Increases in both types of clutter in geospatial displays lead to decreases in search performance for nonexpert participants.[1]

Research has shown that experts perform better on tasks relevant to their area of expertise because they use a more efficient allocation of visual attention.[2] The current research extended this previous research by examining how clutter and expertise affect search performance.

Experimental Design: Thirty-one F/A-18 fighter pilots recruited from various squadrons stationed at Naval Air Station (NAS) Oceana, Virginia, served as our expert group. The pilots were primarily male (28 male, 3 female) with an average age of 30 (range: 25–38, standard deviation (SD) = 4.4) and had an average of 1390 flight hours and 242 combat flight hours. An age-matched control group included 18 NRL participants, primarily scientists. The NRL participants were primarily male (16 male, 2 female) with an average age of 31 (range: 20–49, SD = 6.9) with no flight or navigation background. The stimuli were 72 different base charts with 24 each of low, medium, and high global clutter as shown in Fig. 4. Three different versions of each base chart were created: a target was placed in a region of high local clutter or low local clutter, or the target was absent. The same target symbol was used in each chart, varying only in color in an effort to make the target distinguishable yet similar to other colors in the chart. This control for target saliency is important because a high-contrast target is found quickly regardless of the amount of clutter in the chart.[3]

Low Global Clutter

Medium Global Clutter

High Global Clutter

	L	M	H
Global	2.9	6.1	8.3
Low Local	1.7	4.6	7.0
High Local	4.5	7.3	9.2

Average C3 Values

FIGURE 4
Examples of the low, medium, and high global clutter charts. Black circles indicate the location of high and low local clutter targets. In the versions used in the experiment, only one target was present or no target was present. The black circles are added here to draw attention to the target locations and were not present in the experiment. At bottom right is a table of the average global, low local, and high local C3 clutter values for the low (L), medium (M), and high (H) global clutter charts.

Participants were instructed to determine whether a target was present or absent in each chart. If a participant responded that the target was present, another screen was displayed that instructed him or her to click on the target with the mouse. The chart would appear again and the participant used the mouse to click on the target. If the participant indicated that the target was absent, or a one-minute time-out occurred, the trial ended.

Results: Responses were coded as accurate, inaccurate, or timeout. A 3 × 3 × 2 mixed model analysis of variance (ANOVA) was conducted with three levels of global clutter (high, medium, low), three types of target presence (high, low, absent), and two levels of expertise (pilots, age-matched control) for accuracy and reaction time on accurate trials.

Accuracy: Accuracy was calculated by dividing the number of accurate trials by the number of trials for which a response was given within the one-minute time limit. Experts (i.e., pilots) were significantly more accurate than the control group on the high and medium global clutter trials when the target was in a high local clutter region. The control group was more accurate than the experts on the high global clutter/target absent trials. There were statistical main effects for global clutter and target presence, but not a main effect for expertise (see Fig. 5). However, there were significant interactions between global clutter and expertise, and target presence and expertise, and a three-way interaction among target presence, global clutter, and expertise.

Reaction Time: Experts were slower to respond for low global clutter/target absent trials and slower on the high local trials for both medium and low global clutter. While there were main effects for both global clutter and target presence, there was only a marginal main effect for expertise (see Fig. 6).

Conclusions: Our research indicates that both global and local clutter slow search performance and impair search accuracy. Search impairment is particularly prevalent for high and medium global/high local clutter conditions. Expertise did not improve performance across all trial types. However, when the target was present and difficult to find due to high local clutter and medium to high global clutter, experts were better able to accurately find the target. Although

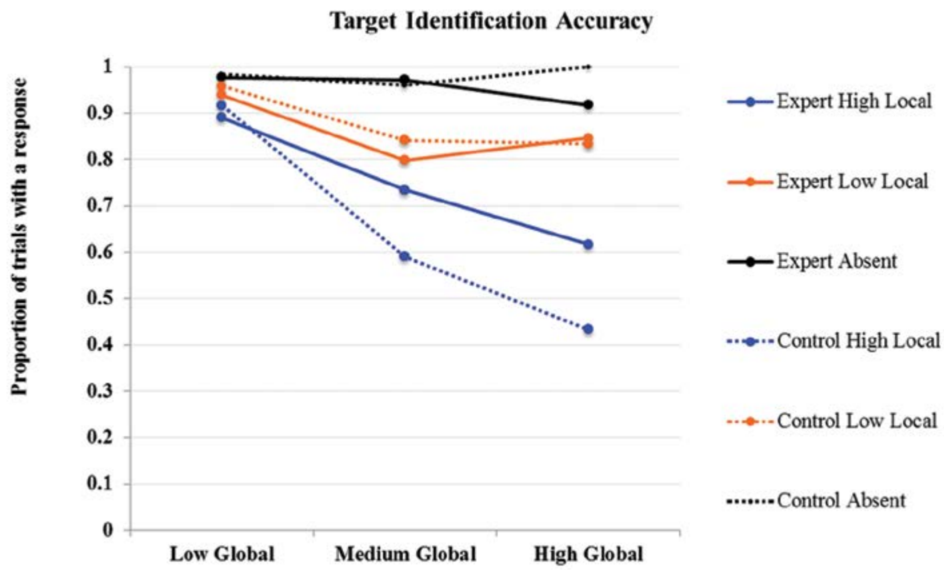

FIGURE 5
Trials in which an accurate response was given within the one-minute time limit.

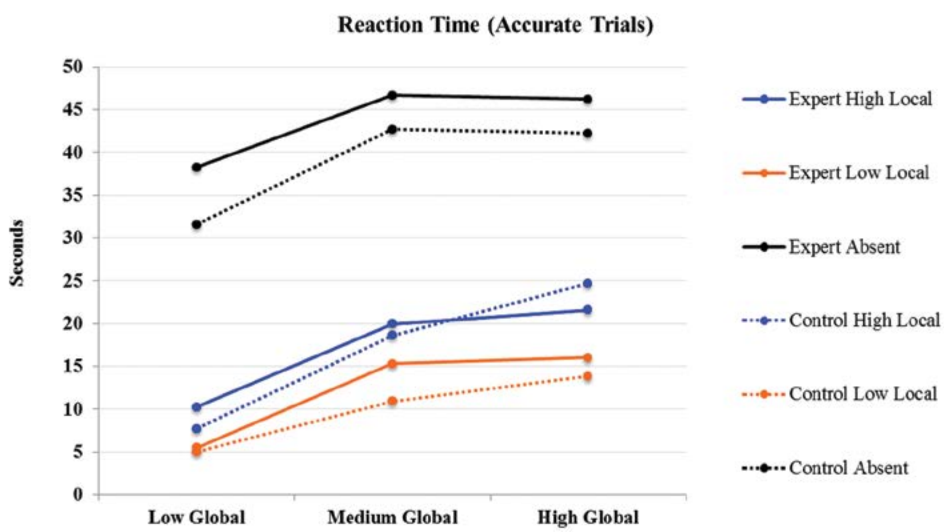

FIGURE 6
Reaction time for accurate trials only.

experts were also slower to respond on the low local/medium global clutter trials, suggesting performance may have improved due to spending more time looking, this was not the case in the high local/high global clutter trials, suggesting that something else may be driving the higher levels of performance on these trials. In addition, analysis of fixation durations and distances between fixations indicate that experts have slightly longer fixation durations, thus taking more time to process information in each fixation. It is not clear if this effect is primarily responsible for the performance improvement in high global/high local clutter conditions.

This research is an important step in deciphering what cognitive processes are at work when extracting information from complex geospatial displays. Further, expertise appears to play a greater role in information retrieval from these displays, particularly as clutter increases. Ultimately, this research can lead to improvements in geospatial display design and improved training doctrine for visual interpretation of these displays.

Acknowledgments: We thank the pilots and navigators at NAS Oceana and the scientists and support personnel at NRL who participated in these experiments. We also thank Ms. Amanda van Lamsweerde and Ms. Rebecca R. Goldstein at Louisiana State University for their help in the gathering and analysis of this data. Finally, we thank Ms. Maura Lohrenz for her vision and guidance on this project as former principal investigator.

[Sponsored by the NRL Base Program (CNR funded)]

References

[1] M.R. Beck, M.C. Lohrenz, and J.G. Trafton, "Measuring Search Efficiency in Complex Visual Search Tasks: Global and Local Clutter," *Journal of Experimental Psychology: Applied* **16**(3), 238–250 (2010).

[2] H.J. Godwin, S.P. Liversedge, J.A. Kirkby, K. Cornes, M. Boardman, and N. Donnelly, "The Influence of Experience upon Threat Assessment and Visual Searching Complex Scenes," poster presented at the annual meeting of the Vision Sciences Society, Naples, FL, May, 2012.

[3] M.R. Beck, M. Trenchard, A. Lamsweerde, R. Goldstein, and M. Lohrenz, "Searching in Clutter: Visual Attention Strategies of Expert Pilots," Proceedings of the Human Factors and Ergonomics Society 54th Annual Meeting, Boston, MA, October 2012, pp. 1411–1415.

♦